ChemComm

PdPt/SrTiO3:Al-catalysed redox-selective photoreduction of unsaturated carboxylic acids using minimal electron-donor and water

Journal:	*ChemComm*
Manuscript ID	CC-COM-07-2024-003791.R1
Article Type:	Communication

COMMUNICATION

PdPt/$SrTiO_3$:Al-catalysed redox-selective photoreduction of unsaturated carboxylic acids using minimal electron-donor and water

Received 00th January 20xx,
Accepted 00th January 20xx

DOI: 10.1039/x0xx00000x

Shogo Mori,*[a] Farzaneh Soleymani Movahed,[b‡] Sha Xue,[b‡] Yuji Sakai,[b] Daling Lu,[c] Takashi Hisatomi,[c] Kazunari Domen,[c,d] Susumu Saito*[a,b]

We developed a semiconductor photocatalyst, Pd-Pt alloy nanoparticle-loaded, Al-doped $SrTiO_3$ (PdPt/STO:Al), for photoreduction of unsaturated carboxylic acids. By the cooperative STO:Al surface and Pd-Pt alloy nanoparticle, the catalyst dispersed in water provided highly redox-selective photoreduction against oxidative degradation of starting materials/products and against reductive evolution of H_2, where minimal glycolic acid worked as an efficient electron-donating fuel.

Semiconductor photocatalysts (SPs) have shown great potential for the realization of green and sustainable chemical reactions. Representative examples include organic pollutant degradation, and more notably, water splitting, where photo-generated holes (h^+s) and electrons (e^-s) promote oxidation of water to O_2 and reduction of protons (H^+s) to H_2 via surface hydrogen species ($H^\bullet = e^- + H^+$), respectively.[1] A vault of modification methods of SPs has been developed, and loading metal nanoparticles on the SP surfaces is one of the most effective strategies to facilitate the generation of the surface $H^\bullet$ for efficient H_2 evolution.[2] For instance, Domen, Hisatomi and their co-workers reported a well-designed SP, Rh-Cr-Co-coloaded, Al-doped $SrTiO_3$ (RhCrCo/STO:Al).[3]

By changing metal nanoparticles on SPs, the reactivity of the surface $H^\bullet$ can be altered for reduction of organic compounds, in which various e^--donors have been used instead of explosive H_2 gas.[4] Although several SPs have been developed for photoreduction, large excess amounts of e^--donors were needed for the quantitative conversion of starting materials.[4–8] It is probably due to competition with oxidative degradation of the organic substrates/products by the h^+s,[5] and/or with the dissipation of the surface $H^\bullet$ for the undesirable H_2 evolution.[6] In other words, the SP-promoted photo-oxidation and reduction were barely controlled. Aiming at a green and sustainable organic synthesis, the use of the organic e^--donors must be rationally reduced,[9] and also water should be used on purpose more effectively.[10]

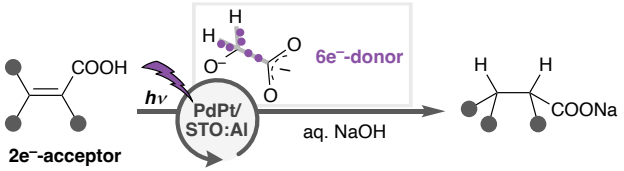

Scheme 1 PdPt/STO:Al-catalyzed redox-selective photoreduction using minimal glycolic acid (GA) and water.

In this work, we newly developed Pd-Pt alloy nanoparticle (ANP)-loaded STO:Al (PdPt/STO:Al) that promotes photoreduction of organic compounds using a minimal[11] e^--donor in water (Scheme 1). For instance, C=C (double) bonds of unsaturated carboxylic acids (CAs), corresponding to $2e^-$-acceptor, were hydrogenated by using minimal glycolic acid (GA) as $6e^-$-donor [C=C bond of **1a**:GA = 3 ($\times$ $2e^-$-acceptor):1 ($\times$ $6e^-$-donor) mol/mol]. PdPt/STO:Al provides highly redox-selective photoreduction,[12] which is promoted exclusively against the oxidative degradation of organic substrates/products, and against the reductive evolution of H_2. Unlike many privileged photo-oxidation of CAs (e.g., decarboxylation) catalyzed by TiO_2,[13–15] photoreduction of CAs predominates in the PdPt/STO:Al system. In addition, CA products are easily isolated by a simple work-up procedure including neutralization with a Brønsted acid and decantation to remove the heterogeneous catalyst. The recovered catalyst was reused for at least four cycles with a minute decrease in the catalytic activity. Besides, PdPt/STO:Al functions under simulated solar light irradiation and in the fully aqueous media without organic solvents.[16] These features are advantageous in many respects for green and sustainable organic synthesis.

We initially studied a series of reactions of **1a** with various SPs under near-UV light irradiation (λ = 365 nm, Fig. S1) to synthesize **2a** in basic water without organic e^--donors (Table 1). Pristine STO:Al did not give **2a** (**2a**: <1%, entry 1). While Pd/STO:Al (1.5 wt% Pd) and Pt/STO:Al (1.5 wt% Pt) gave small

[a] *Integrated Research Consortium on Chemical Sciences, Nagoya University, Chikusa, Nagoya, Aichi 464-8602, Japan E-mail: mori.shogo.n1@f.mail.nagoya-u.ac.jp, saito.susumu.c4@f.mail.nagoya-u.ac.jp*
[b] *Department of Chemistry, Graduate School of Science, Nagoya University, Chikusa, Nagoya, Aichi 464-8602, Japan.*
[c] *Research Initiative for Supra-Materials, Interdisciplinary Cluster for Cutting Edge Research, Shinshu University, Wakasato, Nagano, Nagano, 380-8553, Japan.*
[d] *Office of University Professors, The University of Tokyo, Yayoi, Bunkyo, Tokyo, 113-8656, Japan.*
† Electronic Supplementary Information (ESI) available: Experimental procedures, and characterization of organic compounds and semiconductor photocatalysts. See DOI:
‡ These authors contributed equally to this work.

Table 1 Optimization of the reaction conditions[a]

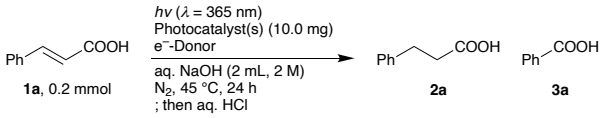

Entry	Photocatalyst (s)	e⁻-Donor	Yield of **2a** (%)	Yield of **3a** (%)
1	STO:Al	–	<1	<1
2	Pd/STO:Al	–	19	<1
3	Pt/STO:Al	–	22	2
4	PdPt/STO:Al	–	55	4
5[b]	Pd/STO:Al and Pt/STO:Al	–	26	3
6	PdPt/STO	–	3	<1
7[cd]	PdPt/STO:Al	–	86±3	5
8[ce]	PdPt/STO:Al	–	86	4
9[cf]	PdPt/STO:Al	–	81	4
10[c]	PdPt/STO:Al	Oxalic acid (0.1 mmol)[i]	68	3
11[c]	PdPt/STO:Al	Glyoxylic acid (0.05 mmol)[j]	88	3
12[cg]	PdPt/STO:Al	GA (0.034 mmol)[k]	>99	<1
13[h]	PdPt/STO:Al	GA (0.34 mmol)	86	1

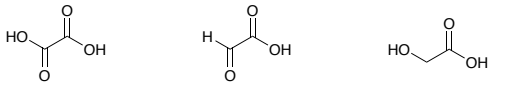

[a] Conditions: **1a** (0.2 mmol), *hν* (*λ* = 365 nm), photocatalyst(s) (10.0 mg), e⁻-donor, aq. NaOH (2 mL, 2 M), N_2, 45 °C, 24 h. Yields were determined by ^{1}H NMR analysis after neutralization by aq. HCl. [b] Photocatalysts (5.0 mg each). [c] **1a** (0.1 mmol). [d] CO_2 (50 μmol) was detected. [e] Simulated solar light, 96 h. [f] In the 4th run of catalyst recycling. [g] CO_2 (30 μmol) was detected. [h] **1a** (1 mmol), 8 h, *hν* (*λ* = 370 nm). [i] 2e⁻-donor. [j] 4e⁻-donor. [k] 6e⁻-donor.

amounts of **2a** (ca. 20%, entries 2 and 3), PdPt/STO:Al (1.5 wt% Pd and Pt) promoted the desirable reaction more efficiently (**2a**: 55%, entry 4). The formation of the Pd-Pt ANPs on STO:Al surfaces was confirmed by a scanning transmission electron microscopy (STEM) with an energy dispersive X-ray spectroscopy (EDX) (Figs. 1a–d). The EDX line scanning profiles obviously demonstrated that Pd and Pt were randomly mixed in the ANPs (Figs. 1a, 1e, and 1f). The high resolution (HR) TEM image showed lattice fringes with *d*-spacings of 0.220 nm and 0.199 nm, assignable to the (111) and (200) planes of the fcc Pd-Pt ANPs, respectively (Fig. 1g).[17,18] When Pd/STO:Al and Pt/STO:Al were used instead of PdPt/STO:Al, a less amount of **2a** was obtained in 26% (entry 5), suggesting that the Pd-Pt ANPs formation on the same STO:Al surface is critical. In a control experiment using PdPt/STO without Al-doping, the hydrogenation hardly proceeded (**2a**: 3%, entry 6). Al-doping would prevent recombination of the photo-generated h^+ and e^- by diminishing recombination sites in the STO lattice, resulting in the enhanced catalytic ability.[3] The yield of **2a** was further increased when 0.1 mmol of **1a** was used (**2a**: 86%, entry 7). PdPt/STO:Al was also driven by a simulated solar light

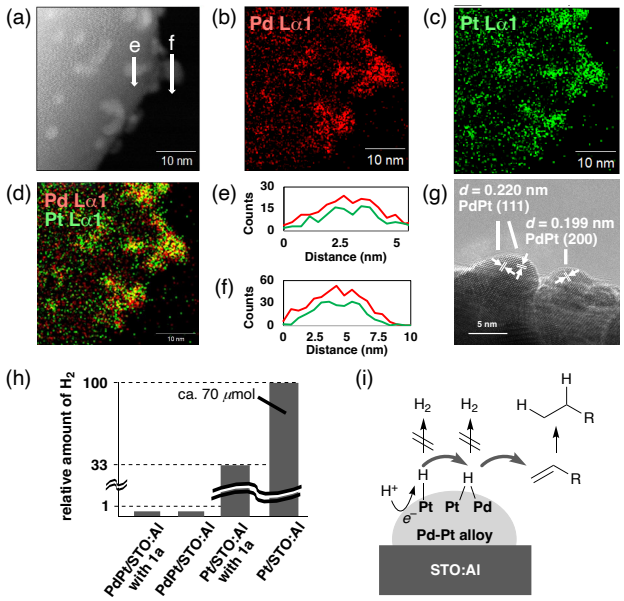

Fig. 1 Pd-Pt ANPs on STO:Al (a) STEM image. STEM-EDX mapping images for (b) Pd (Lα1, red), (c) Pt (Lα1, green), and (d) overlay (overlapped points were highlighted in yellow). (e, f) EDX line scanning profiles. (g) HR-TEM image. (h) H_2 evolution abilities of the photocatalysts. Conditions: *hν* (*λ* = 365 nm), photocatalyst (10.0 mg), GA (ca. 0.035 mmol), aq. NaOH (2 mL, 2 M), N_2, 45 °C, 24 h. (i) Proposed surface H•-relay mechanism. Stoichiometry was omitted for simplicity.

irradiation (**2a**: 86%, entry 8, Fig. S2). Heterogeneous PdPt/STO:Al was easily recovered by centrifugation and decantation after the reaction, and was reused in at least four successive cycles without a significant decrease in the catalytic ability (**2a**: 81% in the 4th run, entry 9, Fig. S4). PdPt/STO:Al recovered after the 4th run was characterized to investigate important factors of the catalytic activity, as will be described later.

Other reaction parameters were optimized as shown in Tables S1–S3. It should be noted that the reaction was promoted in water without base additives, albeit with low efficiency. The use of NaOH was effective for dissolution of **1a** and for dispersion of PdPt/STO:Al in the reaction mixture, resulting in a better reactivity. Control experiments indicated that light irradiation and the photocatalyst are necessitated and that the protocol is robust against the presence of O_2 in air and ions in tap water (Table S4).

According to the liquid- and gas-phase analyses for the reaction using PdPt/STO:Al (entry 7), **3a** (5%) and CO_2 (50 μmol) were detected, while O_2, which is the product of water oxidation, was not generated, indicating that oxidative degradation of **1a** and/or **2a** occurred and the extracted e⁻s therefrom were used for the hydrogenation of **1a**. When benzaldehyde, seemingly derived by the oxidation of **1a**,[19] was used instead of **1a**, benzoic acid (**3a)** was produced (30%) but CO_2 was hardly detected (Scheme S1). In a similar reaction with **2a** as a starting material, no **3a** but CO_2 (30 μmol) was detected (Scheme S2).[13–15] Thus, **1a** and **2a** would be oxidized mainly to **3a** and CO_2, respectively (Scheme S3).

Inspired by a preceding report on the smooth oxidation of lactic acid with H_2 evolution enabled by an interplay of photocatalytic TiO_2-surfaces and loaded Pt nanoparticles,[20] we envisioned that selective oxidation of α-hydroxycarboxylic acid or its structural analogues, which more strongly bind to the SP surface, would outperform undesirable oxidation of **1a** and **2a** by a similar synergistic effect of STO:Al surfaces and Pd-Pt ANPs (entries 10–12). Finally, GA was found to be a competent e^--donor: **1a** was converted into **2a** exclusively when minimal GA was used (**2a**: >99%, **3a**: <1%, C=C bond:GA = 3:1 mol/mol, entry 12).[11] At the same time, CO_2 (30 μmol) was detected.[21] We also conducted a similar reaction using D_2O instead of H_2O. A post-reaction sample of the D_2O phase was analyzed by ^1H NMR immediately after solid residues were filtrated, where GA and relevant small organic molecules derived therefrom were undetected (Fig. S5). These observations indicate that GA functioned as the efficient 6e^--donor. The D-labeling experiment also suggested that water was the source of two H^+s incorporated into the hydrogenated product (Fig. S5, Table S7).[22–24] A more scalable reaction (**1a**, 1 mmol) was successful (**2a**: 86% entry 13, Fig. S3, Table S5).

To get further insights into the function of the Pd-Pt ANPs, H_2 evolution abilities among photocatalysts were compared (Fig. 1h). The detection of H_2 was negligible under the standard conditions using PdPt/STO:Al and **1a**. In the absence of **1a**, PdPt/STO:Al hardly produced H_2 as well. In contrast, Pt/STO:Al produced relatively large amounts of H_2 both in the presence and absence of **1a**. These observations could be interpreted as follows (Fig. 1i): A photo-excited e^- of PdPt/STO:Al accommodated at a Pt site, whose work function is larger than that of Pd,[25] would reduce a H^+ to a surface $H^\bullet$ at the Pt site (Pt–H). While the Pt–H is prone to be consumed for H_2 evolution, it would also be possible to be transferred to an interface between Pt and Pd in the ANP, which can store a higher concentration of $H^\bullet$ than the Pt site.[26] The formed Pd–H–Pt would be used dominantly for the hydrogenation of the C=C bond of **1a** that outclasses the undesirable H_2 evolution. Similar surface $H^\bullet$-relay mechanisms involving Pd-Pt ANPs loaded on other SP surfaces were also proposed previously.[7,8]

Overall, the smooth and selective e^- transfer from GA to **1a** would be promoted by the cooperative role of STO:Al surfaces and the Pd-Pt ANPs: GA would be oxidized through the interplay of the STO:Al surfaces and Pd-Pt ANPs, followed by reduction of **1a** through the surface $H^\bullet$-relay mechanism on the Pd-Pt ANPs.

Under the established standard conditions, a variety of C=C- or C≡C (triple) bonds of CAs were photocatalytically hydrogenated efficiently and selectively (Fig. 2a). *Trans*-cinnamic acids containing an electron-donating, an electron-withdrawing or a sterically demanding substituent underwent the hydrogenation smoothly (**2b**–**2d**: ≥90%). The hydrogenation took place efficiently even when the olefin moiety was not directly π-conjugated with the carboxyl group (**2e**: 71%). A CA with a C≡C bond (**1f**) was doubly hydrogenated to **2a** using minimal GA within 24 h [**2a**: 95%, C≡C bond:GA = 3 ($\times$ 4e^--acceptor):2 ($\times$ 6e^--donor) mol/mol]. Just by shortening the reaction time to 6 h, a partially hydrogenated product with a *cis*-configuration was obtained selectively (**1a'**: 70%).

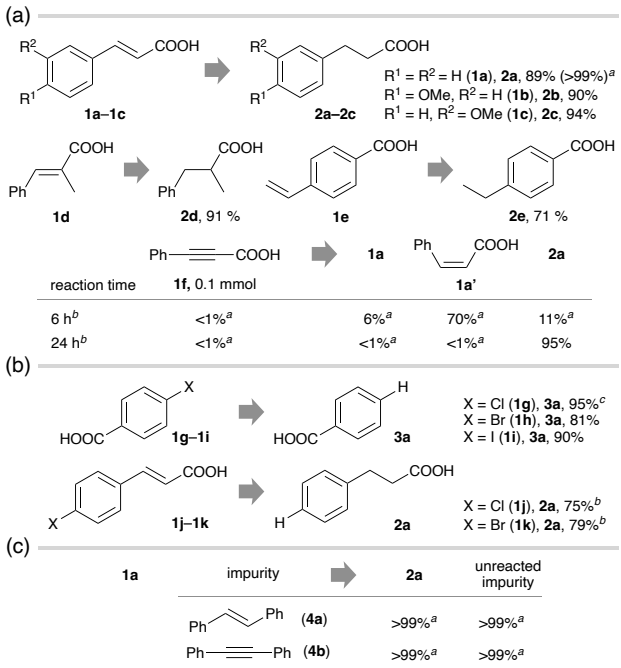

Fig. 2 Generality and chemoselectivity. (a) Hydrogenation. (b) Hydrodehalogenation. (c) Chemoselective hydrogenation in the presence of impurity (0.1 mmol). Conditions: unsaturated CA (**1**, 0.1 mmol), *hv* (λ = 365 nm), PdPt/STO:Al (10.0 mg), GA (ca. 0.035 mmol), aq. NaOH (2 mL, 2 M), N_2, 45 °C, 24 h. Isolated yield after neutralization by aq. HCl. [a] Determined by ^1H NMR analysis after neutralization by aq. HCl. [b] GA (ca. 0.07 mmol). [c] 30 h.

Cl, Br and I-substituted benzoic acids (**1g**–**1i**) underwent photocatalytic hydrodehalogenation (substitution of halogens with hydrogen) under the PdPt/STO:Al system (**3a**: >80%, Fig. 2b). Accordingly, CAs with a C=C bond and a C(sp^2)–Cl or a C(sp^2)–Br bond (**1j** and **1k**) provided uniformly the doubly hydrogenated product (**2a:** ≥75%).

Emphasis should be placed on the ease of isolation of the products. The desirable products, which were formed cleanly, could be isolated with analytically high purities just by a simple work-up procedure including neutralization by an aqueous solution of HCl and extraction, without column chromatography.

As demonstrated above, CAs soluble in water were competent substrates, while non-polar chemicals with a C=C bond (**4a**) or with a C≡C bond (**4b**) remained largely intact (Scheme S4). Even in the presence of non-polar **4a** or **4b**, water-soluble **1a** with the carboxyl group underwent the hydrogenation chemoselectively while **4a** and **4b** were hardly hydrogenated (Fig. 2c).

The newly developed PdPt/STO:Al was characterized by several spectroscopic and microscopic techniques. By inductively coupled plasma-atomic emission spectroscopy (ICP-AES), the metal composition of PdPt/STO:Al was determined to be 1.38 wt% for Pd and 1.27 wt% for Pt. X-ray photoelectron spectroscopy (XPS) showed that freshly prepared PdPt/STO:Al mainly contains Pd^0 and Pt^0 rather than Pd^{2+}, Pt^{2+} and Pt^{4+} (Figs. S6a and d). The binding energies for Pd^0 3*d* and Pt^0 4*f* of

PdPt/STO:Al were lower than the standard values of bulk Pd^0 and Pt^0, suggesting electronic interactions of both Pd and Pt with STO:Al. The TEM image of PdPt/STO:Al showed that fine Pd-Pt ANPs were randomly dispersed on all the STO:Al surfaces since the ANPs were loaded by the standard impregnation method (Figs. S7a). Other characterization data of PdPt/STO:Al were shown in Figs. S8 and S9.

In the catalyst recycling experiments, the photocatalytic ability was slightly decreased through each run (Fig. S4). The possible causes of a gradual deactivation of the catalyst: (i) leaching of the Pd-Pt ANPs from the STO:Al surfaces; (ii) changes of the electronic properties (formal charges) of Pd and/or Pt; and (iii) aggregation of the ANPs were investigated. (i) The ICP-AES analysis demonstrated that Pd and Pt were scarcely leached into solutions even after the 4th cycle (1.35 wt% Pd, 1.24 wt% Pt) compared with the initial state (1.38 wt% Pd, 1.27 wt% Pt). (ii) The XPS analysis of PdPt/STO:Al recovered after the 4th run showed that oxidized Pd^{2+} and Pt^{4+} were dominant species rather than Pd^0 or Pt^0 (Figs. S6b and e). Although the oxidation states of Pd and Pt of the recovered PdPt/STO:Al were restored to their initial states by reduction with $NaBH_4$ (Figs. S6c and f), the photocatalytic ability could not be refreshed (Table S6). These results suggested that the oxidation states of Pd and Pt would not be important for the photocatalytic performance. (iii) According to the XPS analysis, the surface atomic ratio of Pd and Pt relative to Ti were decreased after the 4th run, implying that the fine Pd-Pt ANPs would aggregate (before reaction: Pd/Ti = 0.48, Pt/Ti = 0.34; after the 4th run: Pd/Ti = 0.27, Pt/Ti = 0.30). In the TEM image of the PdPt/STO:Al recovered after the 4th run, most of the fine Pd-Pt ANPs disappeared and relatively large Pd-Pt ANPs were mainly observed (Fig. S7b). Therefore, we can conclude that the aggregation of the Pd-Pt ANPs negatively affected the photocatalytic performance.

In summary, the redox-selective reduction of organic compounds was enabled by a newly developed PdPt/STO:Al photocatalyst with minimal GA as the e^--donor in water. Selective e^--transfer from GA to CAs would be enabled by the cooperation of the STO:Al surfaces and the Pd-Pt ANPs. This study demonstrates the great potential of ANPs-loaded SPs for clean and selective organic synthesis directed toward sustainable material production.

This work was partially supported by MEXT/JSPS Grant-in-aid for Early-Career Scientists, Specially Promoted Research, Transformative Research Areas (A): Green Catalysis, and International Leading Research, KAKENHI (Grant # 24K17676 to SM, 23H05404, 23H04904, and 22K21346 to SS). This work was also partially supported by JST CREST (Grant # JPMJCR22L2 to SS), Yashima Environment Technology Foundation (to SM), Iketani Science and Technology Foundation (to SM), The Naito Research Grant (to SM), Foundation of Public Interest of Tatematsu (to SM), and the Asahi Glass Foundation (step-up grant to SS). STEM and XPS measurements were performed by Kimitaka Higuchi (Nagoya U) and Michiko Obata (Shinshu U), respectively. We thank Dr. Satoshi Muratsugu (Nagoya U) and Dr. Satoru Ikemoto (Nagoya U) for insightful discussions.

Conflicts of interest

There are no conflicts to declare.

Data availability

The data supporting this article have been included as part of the Supplementary Information.

Notes and references

1 Q. Wang and K. Domen, *Chem. Rev.*, 2020, **120**, 919.
2 K. Wenderich and G. Mul, *Chem. Rev.*, 2016, **116**, 14587.
3 T. Takata, J. Jiang, Y. Sakata, M. Nakabayashi, N. Shibata, V. Nandal, K. Seki, T. Hisatomi and K. Domen, *Nature*, 2020, **581**, 411.
4 D. Ma, S. Zhai, Y. Wang, A. Liu and C. Chen, *Molecules*, 2019, **24**, 330.
5 A. Kinoshita, K. Nakanishi, R. Yagi, A. Tanaka, K. Hashimoto and H. Kominami, *Appl. Catal., A*, 2019, **578**, 83.
6 K. Nakanishi, R. Yagi, K. Imamura, A. Tanaka, K. Hashimoto and H. Kominami, *Catal. Sci. Technol.*, 2018, **8**, 139.
7 M. Li, N. Zhang, R. Long, W. Ye, C. Wang and Y. Xiong, *Small*, 2017, **13**, 1604173.
8 Y. Shiraishi, Y. Takeda, Y. Sugano, S. Ichikawa, S. Tanaka and T. Hirai, *Chem. Commun.*, 2011, **47**, 7863.
9 C. R. McElroy, A. Constantinou, L. C. Jones, L. Summerton and J. H. Clark, *Green Chem.*, 2015, **17**, 3111.
10 M. Yamauchi, H. Saito, T. Sugimoto, S. Mori and S. Saito, *Coord. Chem. Rev.*, 2022, **472**, 214773.
11 The "minimal" e^-s for reduction of a C=C bond are two. The number of e^-s provided by an organic e^- donor can be counted as 2 × the number of C–H and C–C bonds available from an e^- donor. Stable C–O bonds cannot be used as e^- sources. The e^- donor is finally converted into CO_2, representing the fully oxidized/oxygenated form of carbon.
12 Z. Liu, J. Caner, A. Kudo, H. Naka and S. Saito, *Chem. Eur. J.*, 2013, **19**, 9452.
13 Q. Zhu and D. G. Nocera, *J. Am. Chem. Soc.*, 2020, **142**, 17913.
14 D. W. Manley, R. T. McBurney, P. Miller, R. F. Howe, S. Rhydderch and J. C. Walton, *J. Am. Chem. Soc.*, 2012, **134**, 13580.
15 Z. Huang, Z. Zhao, C. Zhang, J. Lu, H. Liu, N. Luo, J. Zhang and F. Wang, *Nat. Catal.*, 2020, **3**, 170.
16 F. Zhou, Z. Hearne and C.-J. Li, *Curr. Opin. Green Sustainable Chem.*, 2019, **18**, 118.
17 Q. Yang, L. Shi, B. Yu, J. Xu, C. Wei, Y. Wang and H. Chen, *J. Mater. Chem. A*, 2019, **7**, 18846.
18 H. Dai, T. Zhang, H. Pu, K. Dong, Y. Wang and Y. Deng, *Appl. Surf. Sci.*, 2022, **602**, 154318.
19 X. Li, Q. Wang, J. Lyu and X. Li, *ChemistrySelect*, 2021, **6**, 9735.
20 K. Liu, A. Litke, Y. Su, B. G. Van Campenhout, E. A. Pidko and E. J. M. Hensen, *Chem. Commun.*, 2016, **52**, 11634.
21 The experimental value of the detected CO_2 (30 μmol) was lower than the theoretical value (ca. 70 μmol). This discrepancy might be because a portion of the generated CO_2 was dissolved in the aqueous media.
22 C. Liu, Z. Chen, C. Su, X. Zhao, Q. Gao, G.-H. Ning, H. Zhu, W. Tang, K. Leng, W. Fu, B. Tian, X. Peng, J. Li, Q.-H. Xu, W. Zhou and K. P. Loh, *Nat. Commun.*, 2018, **9**, 80.
23 E. Zhao, W. Zhang, L. Dong, R. Zboril and Z. Chen, *ACS Catal.*, 2023, **13**, 7557.
24 H. Sun, W. Ou, L. Sun, B. Wang and C. Su, *Nano Res.*, 2022, **15**, 10292.
25 H. B. Michaelson, *J. Appl. Phys.*, 1977, **48**, 4729.
26 M. Yamauchi, H. Kobayashi and H. Kitagawa, *ChemPhysChem*, 2009, **10**, 2566.

Data availability

The data supporting this article have been included as part of the Supplementary Information.